

# Identification of system matrices based on experimental modal analysis and its application in structural health monitoring

Sifeng Bi

*Research Associate, Institute for Risk and Reliability, Leibniz Universität Hannover, Hanover, Germany*

Michael Beer

*Professor, Institute for Risk and Reliability, Leibniz Universität Hannover, Hanover, Germany*

Morvan Ouisse, Emmanuel Foltête

*Professor, Department of Applied Mechanics, FEMTO-ST Institute, Besancon, France*

**ABSTRACT:** This paper presents a system matrices identification approach directly from the real-time measured structural responses. Based on the experimental modal analysis, the identified system matrices are expected to represent the system behaviours as same as the experimentally measured ones. Due to the fact that the system matrices, i.e. the mass, stiffness, and damping matrices, are the direct reflection of the inherent properties of the structure, they can be naturally served as the indicator of structural damages. The identification approach utilizes the state space representation for the equation development to construct the system matrices using the complex modes (i.e. the complex eigenvalues and eigenvectors). The complex modes, however, requires a calibration process to enforce the so-called properness condition, which is not generally fulfilled by the modes because of the inevitable experimental noise. An efficient method based on the Riccati equation is proposed to calibrate the complex eigenvectors so that they can be safely used to construct the system matrices. A scalar quantity based on the norm of the matrices is defined as the indicator for structural health monitoring. The overall approach is performed on a numerical model of a structure with controllable modifications (i.e. artificial damages). The difference between the identified matrices of the original and modified structures clearly demonstrates the approach's feasibility in structural health monitoring.

## 1. INTRODUCTION

The modern structure systems in civil and mechanical engineering are designed to meet long-term requirements related to structural safety, robustness, and durability. Structural health monitoring (SHM) is continuously a critical issue to monitor, control, and maintain the physical properties of the structure during its overall life-cycle.

The vibration-based damage detection is one of the classical SHM techniques, which follows the principle that the damages would lead to the change of the structural response during the vibration test. The change of the structural response can occur in time, frequency, and modal domains (Carden and Fanning 2004). Consequently, the vast literature on vibration-

based SHM can be classified according to which output feature is investigated as the damage indicator. For example, the direct response in time domain of a situ bridge is investigated via the singular spectrum analysis with the band-pass filter technique to extract the bridge frequencies (Yang et al. 2013). It is more popular to investigate the features in frequency and modal domains, e.g. the frequency response function (FRF), natural frequencies, and modal shapes. A substructure-based FRF approach is proposed by Lin et al. to not only detect but also locate the damage of civil buildings. For the application of modal parameters, Chang and Kim propose to employ multiple modal assurance criteria (MAC) and coordinate MAC values during SHM for a real-scale steel truss bridge.

No matter what kind of feature is investigated in SHM, it is important to make sure that this investigated feature is sensitive to the potential damage. However, the commonly utilized nature frequency, modal shape, and FRFs are not generally sensitive to all damages. In this work, a system matrix identification approach is proposed to identify (i.e. reconstruct) the mass, stiffness, and damping matrices based on the real-time measured FRFs. The structural system matrices are expected to represent the inherent properties of the structures, and thus can be naturally proposed as the damage indicator during SHM.

The matrix identification procedure contains a series of modal analysis techniques. First, the structural dynamic eigenvalue problem is presented by the state space representation, where the inverse procedure from the complex modes (eigenvalues and eigenvectors) to the system matrices are developed. Second, the inverse procedure is valid only if the so-called properness condition (Balmès 1997; Bi et al. 2017) of the complex modes is fulfilled. Hence a calibration process of the modes is required prior to utilizing the modes to reconstruct the system matrices. Finally, a scalar quantity assessing the steadiness of the system matrices is defined to be served as the SHM indicator.

A finite element (FE) model of a free-free conditional beam is utilized in the example part, where a specially designed artificial damage is applied to the FE model. The FRFs and natural frequencies are found to be insensitive to the artificial damage, while the feasibility of the proposed indicator based on the system matrices is demonstrated.

## 2. THEORIES AND METHODS

### 2.1. Inverse procedure for matrix identification

The identification of the system matrix starting from the complex modes (eigenvalues and eigenvectors) is termed as the “inverse procedure”, since it contrasts with the normal “forward procedure” to calculate the complex modes using the existing matrices. The forward

procedure is essentially a second order eigenvalue problem expressed as

$$(\mathbf{M}\lambda_i^2 + \mathbf{C}\lambda_i + \mathbf{K})\boldsymbol{\varphi}_i = 0, i = 1, 2, \dots, n, \quad (1)$$

where  $\mathbf{M}$ ,  $\mathbf{C}$ , and  $\mathbf{K}$  are the mass, damping, and stiffness matrices of the structural system, respectively;  $\lambda_i$  and  $\boldsymbol{\varphi}_i$  are respectively the  $i$ -th eigenvalue and eigenvector;  $n$  is the number of modes.

Considering the state space representation, let  $\mathbf{U} = \begin{bmatrix} \mathbf{C} & \mathbf{M} \\ \mathbf{M} & \mathbf{0} \end{bmatrix}$ ,  $\mathbf{A} = \begin{bmatrix} -\mathbf{K} & \mathbf{0} \\ \mathbf{0} & \mathbf{M} \end{bmatrix}$ ,  $\boldsymbol{\sigma}_i = \begin{bmatrix} \boldsymbol{\varphi}_i \\ \boldsymbol{\varphi}_i\lambda_i \end{bmatrix}$ . The state space representation of Eq. (1) is

$$\begin{aligned} (\mathbf{U}\lambda_i - \mathbf{A})\boldsymbol{\sigma}_i &= 0; \\ (\mathbf{U}\bar{\lambda}_i - \mathbf{A})\bar{\boldsymbol{\sigma}}_i &= 0. \end{aligned} \quad (2)$$

where  $\bar{\boldsymbol{\sigma}}$  is the conjugation of the complex modes. Put these total  $n$  modes into a uniform matrix, and one gets a diagonal eigenvalue matrix  $\boldsymbol{\Lambda} = \begin{bmatrix} \ddots & & \\ & \lambda_i & \\ & & \ddots \end{bmatrix}$  and a eigenvector matrix  $\boldsymbol{\Phi} = [\boldsymbol{\varphi}_1 \ \boldsymbol{\varphi}_2 \ \dots \ \boldsymbol{\varphi}_n]$ . Similar as  $\mathbf{M}$ ,  $\mathbf{C}$ , and  $\mathbf{K}$ ,  $\boldsymbol{\Lambda}$  and  $\boldsymbol{\Phi}$  can also be assembled into the state space representation using the following matrices

$$\boldsymbol{\Upsilon} = \begin{bmatrix} \boldsymbol{\Lambda} & \mathbf{0} \\ \mathbf{0} & \bar{\boldsymbol{\Lambda}} \end{bmatrix}, \boldsymbol{\Sigma} = \begin{bmatrix} \boldsymbol{\Phi} & \bar{\boldsymbol{\Phi}} \\ \boldsymbol{\Phi}\boldsymbol{\Lambda} & \bar{\boldsymbol{\Phi}}\bar{\boldsymbol{\Lambda}} \end{bmatrix}. \quad (3)$$

Then the matrix form of the second-order eigenvalue problem is expressed as

$$\mathbf{U}\boldsymbol{\Sigma}\boldsymbol{\Upsilon} - \mathbf{A}\boldsymbol{\Sigma} = \mathbf{0}. \quad (4)$$

Considering the orthogonality among each eigenvector, a diagonal matrix with  $2n$  arbitrary real values  $\boldsymbol{\Xi} = \begin{bmatrix} \ddots & & \\ & \xi_i & \\ & & \ddots \end{bmatrix}$ ,  $i = 1, \dots, 2n$ , is necessary to rewrite Eq. (4) as

$$\begin{aligned} \boldsymbol{\Sigma}^T \mathbf{U} \boldsymbol{\Sigma} &= \boldsymbol{\Xi}, \\ \boldsymbol{\Sigma}^T \mathbf{A} \boldsymbol{\Sigma} &= \boldsymbol{\Xi} \boldsymbol{\Upsilon}. \end{aligned} \quad (5)$$

Since  $\boldsymbol{\Xi}$  is an arbitrary matrix, without loss of generality, the identify matrix  $\mathbf{I}$  can be proposed to instead  $\boldsymbol{\Xi}$  in Eq. (5), and thus the following expresses are obtained:

$$\begin{aligned} \mathbf{U}^{-1} &= \boldsymbol{\Sigma} \boldsymbol{\Sigma}^T, \\ \mathbf{A}^{-1} &= \boldsymbol{\Sigma} \boldsymbol{\Upsilon}^{-1} \boldsymbol{\Sigma}^T. \end{aligned} \quad (6)$$

Transfer the  $2n$  Degree of Freedom (DoF) state space representation back to the  $n$ -DoF

physical system presentation, Eq. (6) is rewritten as

$$\begin{bmatrix} \mathbf{C} & \mathbf{M} \\ \mathbf{M} & \mathbf{0} \end{bmatrix}^{-1} = \begin{bmatrix} \Phi\Phi^T & \Phi\Lambda\Phi^T \\ \Phi\Lambda\Phi^T & \Phi\Lambda^2\Phi^T \end{bmatrix},$$

$$\begin{bmatrix} -\mathbf{K} & \mathbf{0} \\ \mathbf{0} & \mathbf{M} \end{bmatrix}^{-1} = \begin{bmatrix} \Phi\Lambda^{-1}\Phi^T & \Phi\Phi^T \\ \Phi\Phi^T & \Phi\Lambda\Phi^T \end{bmatrix} \quad (7)$$

The expressions of  $\mathbf{M}$ ,  $\mathbf{C}$ , and  $\mathbf{K}$  can be easily extracted as

$$\begin{cases} \mathbf{M} = [\Phi\Lambda\Phi^T]^{-1} \\ \mathbf{C} = -[\mathbf{M}(\Phi\Lambda^2\Phi^T)\mathbf{M}]. \\ \mathbf{K} = -[\Phi\Lambda^{-1}\Phi^T]^{-1} \end{cases} \quad (8)$$

Eq. (8) is the so-called inverse procedure, where the mass, damping, and stiffness matrices are exclusively determined by the complex eigenvalues and eigenvectors. Note that, the conjugations of the modes in Eqs. (7) and (8) have been omitted for layout clarity. However, these conjugation parts should not be ignored during the practical evaluation of both the inverse procedure and the following properness condition enforcement procedure.

### 2.2. Properness condition enforcement

The previous subsection presents the inverse procedure to reconstruct the system matrices using the complex modes. However, an importance pre-condition must be first fulfilled by the modes, before they can be utilized in the inverse procedure. From Eq. (7), this pre-condition can be easily extracted as

$$\Phi\Phi^T = \mathbf{0}. \quad (9)$$

This pre-condition is first denominated as “properness condition” by Balmès, however, this concept has been investigated with various terminologies in the literatures (Bernal and Gunes 2000; Lancaster and Prells 2005; Zhang and Lallement 1987). In the ideal case when there is no noise, the theoretically exact modes can fulfill the properness condition automatically. However, since the experimental noise and uncertainty are inevitable, the experimentally identified modes generally cannot fulfill this condition, leading the directly constructed system matrices far from the

physical ones. Hence, a critical step for matrix identification is to enforce the properness condition of the modes, before they can be safely utilized in the inverse procedure.

The properness condition enforcement process can be expressed as an optimization problem, where the optimal object is an approximate  $\tilde{\Phi}$ ; the objective function is  $g(\Phi) = \|\tilde{\Phi} - \Phi\|$ ; and the constraint is  $\tilde{\Phi}\tilde{\Phi}^T = \mathbf{0}$ . A direct solution of this problem is difficult, since the optimal object  $\tilde{\Phi}$  is a matrix with complex value for each element leading to a large number of optimal parameters, and subsequently a huge calculation cost. Alternatively, Balmès proposed another technique to solve this problem by determining the Lagrange multiple matrix  $\delta$  within the Riccati equation

$$\Phi\Phi^T - \delta\bar{\Phi}\Phi^T - \delta\Phi\bar{\Phi}^T + \delta\bar{\Phi}\bar{\Phi}^T\delta = \mathbf{0}. \quad (10)$$

After  $\delta$  is obtained, the approximate  $\tilde{\Phi}$  can be calculated following

$$\tilde{\Phi} = [\mathbf{I} - \delta\bar{\delta}]^{-1}[\Phi - \delta\bar{\Phi}]. \quad (11)$$

Compared with the optimization approach, the technique using Eqs. (10) and (11) is more efficient with significantly reduced calculated cost. After the properness condition enforcement, however, the approximate eigenvector  $\tilde{\Phi}$  can only be utilized to construct the mass and stiffness matrix. The damping matrix obtained from Eq. (8) is still far from the physical one, because of its high sensitivity to the noise and uncertainty in both eigenvalues and eigenvectors. For the further treatment of the damping identification within this inverse procedure, the readers are suggested to refer to (Bi et al. 2018) for a probabilistic approach to deal with this challenging damping identification with the consideration of experimental uncertainty. Nevertheless, the stiffness and mass matrices are enough for the current application to reveal the damage of the structural system, as long as these properties are precisely identified.

### 2.3. Assessment of matrix change for SHM

Since the mass and stiffness matrices are directly identified from the real-time measured system

behaviors, the matrices are sensitive to any change of the structure properties, and consequently they can be used to indicate the structure fatigue and failure. The change of the matrix can be quantified using the 2-norm of the matrix:

$$i = \frac{\|\hat{\mathbf{A}} - \mathbf{A}\|}{\|\mathbf{A}\|} \times 100 \quad (12)$$

where  $\mathbf{A}$  is the mass or stiffness matrix identified from the original undamaged structure;  $\hat{\mathbf{A}}$  is the matrix identified from the real-time measured response of the structure under serving condition. When the structural system is undamaged, the SHM index  $i$  is close to zero; when fatigue or damage occurs, the SHM index  $i$  would increase. The performance of this proposed SHM index is demonstrated in the following example part.

### 3. EXAMPLE

#### 3.1. Problem description

A simulated example is proposed in this section employing a numerical model of an aluminium

beam with periodic thickness and a free-free condition. The FE model of the beam as well as its geometry details is shown in Figure 1. A harmonic excitation with uniform load is added on the right top to simulate the practical vibration test. Five measurement points (corresponding to sensors in real experiment) are assigned distributing along the centre line of the beam, denoted as measurement points #1-#6 in Figure 1. The distances from the left top to these measurement points are 28 mm, 281 mm, 431 mm, 581 mm, 781 mm, and 1066 mm, respectively. A real experimental setup has been utilized by (Bi et al. 2018). However, the current work only employs the simulated model with the purpose for an explicit control of the artificial damage on this beam. For the damaged case, two modification points are applied to the FE model on the elements associating to measurement points #2 and #5.

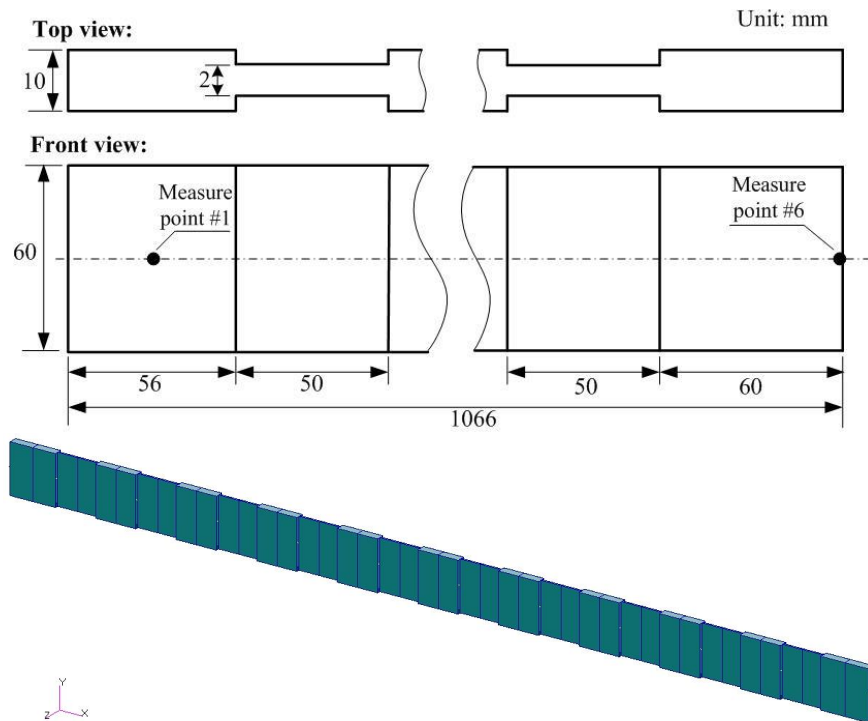


Figure 1 The geometry details and the FE model of the beam

The general strategy in this simulated example is explained as follows.

1. Run a FE analysis using the original beam model, and obtain the original FRFs;
2. Identify the complex modes from the original FRFs, and construct the system matrices following the inverse procedure as described in Section 2.1;
3. Apply the modifications to FE model on the certain elements; that is to say, add artificial damage on the beam;
4. Repeat Steps 1 and 2 to obtain the modified system matrices, and check the differences between the two sets of matrices using the assessment indicator defined in Section 2.3.

In the following context, the two sets of data (i.e. the FRFs, complex modes, and system matrices) before and after adding damage are designated after *Original* and *Modified*, respectively. The original and modified properties of the FE model are detailed in Table 1. In the following section, a detailed comparison between the original and modified data is presented to assess how much the final system matrices can be changed by the artificial damage.

Table 1 Parameters of the original model and two modification points of the modified model

|                      | Original | Modified |          |
|----------------------|----------|----------|----------|
|                      |          | Point #1 | Point #2 |
| $E (10^{10} Pa)$     | 7        | 9        | 5        |
| $\rho (10^3 Kg/m^3)$ | 2.7      | 3.47     | 1.93     |

### 3.2. Comparison of the natural frequencies and FRFs

The natural frequencies before and after the modification are listed in Table 2. It is interesting to found that, although significant modifications are applied to the beam, its natural frequencies are not obviously changed. The absolute mean error of the frequencies of the modified beam, according to the original ones, is only 0.656%, implying the natural frequencies are insensitive to the artificial damage.

Table 2 The natural frequencies of the original and modified beams

| Natural frequency (Hz) | Original | Modified*     |
|------------------------|----------|---------------|
| $f_1$                  | 6.949    | 6.879 (-1.00) |
| $f_2$                  | 19.41    | 19.13 (-1.46) |
| $f_3$                  | 38.50    | 38.33 (-0.42) |
| $f_4$                  | 64.45    | 64.44 (-0.02) |
| $f_5$                  | 97.54    | 96.84 (-0.71) |
| $f_6$                  | 138.9    | 138.4 (-0.32) |
| Absolute mean error    |          | 0.656%        |

\*percent error according to the original data in the parentheses

Besides the natural frequencies, the FRFs are typically employed to indicate the property change of the structures in the iteration. However, as shown in Figure 2 and Figure 3, the FRFs keep unchanged after the modifications are applied to the beam. The nearly identical FRF curves in the figures and the extremely small error in Table 2 demonstrate that neither the FRF nor the natural frequency is capable of monitoring the artificial damage in this example. Alternatively, the performance of the reconstructed system matrices is assessed in the following subsection.

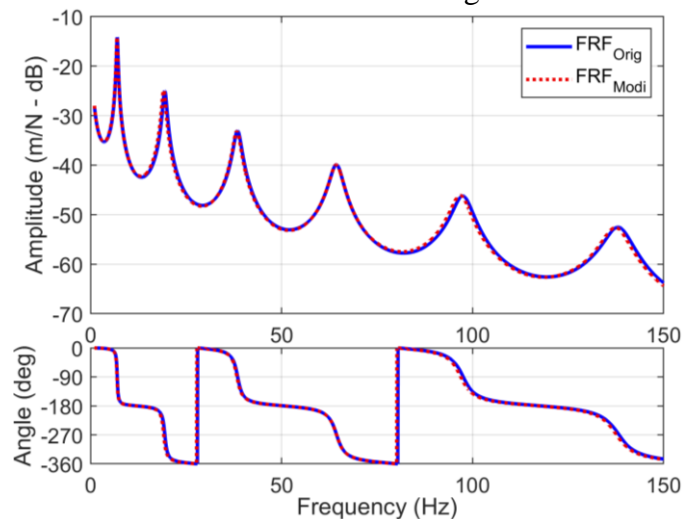


Figure 2 The FRFs at measurement point #1 before and after the modifications

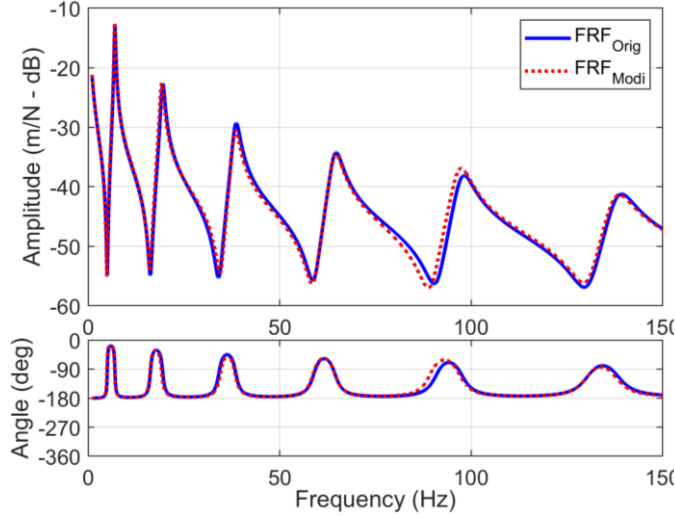


Figure 3 The FRFs at measurement point #6 before and after the modifications

### 3.3. Comparison of the system matrices

After the inverse procedure and properness enforcement, the reconstructed system matrices are utilized in this subsection to indicate the property change of the structure. The stiffness matrices before and after the modification,  $K_{orig}$  and  $K_{modi}$ , are listed as follows.

$$K_{orig} = \begin{bmatrix} 606 & 614 & 303 & 291 & 227 & 17.9 \\ 614 & 990 & 179 & 449 & 418 & 118 \\ 303 & 179 & 462 & 4.95 & 151 & 33.9 \\ 291 & 449 & 4.95 & 537 & 332 & 205 \\ 227 & 418 & 151 & 332 & 721 & 301 \\ 17.9 & 118 & 33.9 & 205 & 301 & 230 \end{bmatrix}$$

$$K_{modi} = \begin{bmatrix} 657 & 726 & 292 & 342 & 229 & 18.8 \\ 726 & 1233 & 163 & 554 & 432 & 122 \\ 292 & 163 & 458 & -9.7 & 120 & 22.3 \\ 342 & 554 & -9.7 & 588 & 322 & 203 \\ 229 & 432 & 120 & 322 & 600 & 262 \\ 18.8 & 122 & 22.3 & 203 & 262 & 216 \end{bmatrix}$$

The SHM index  $i$  of the stiffness matrix is calculated as  $i_k = \frac{\|K_{modi} - K_{orig}\|}{\|K_{orig}\|} \times 100 = 16.6\%$ .

Similarly, the SHM indices of the mass matrix is 7.43%. The system matrices of the modified FE model are clearly different from the ones of the original FE model, implying the identified system matrices can serve as an effective indicator of the artificial damage in this example.

## 4. CONCLUSION

This work presents an inverse procedure to identify the system matrix from the real-time measured response of the structural system. The properness enforcement method is utilized to calibrated the complex modes, such that the identified matrices can represent the system behaviours as same as the experimentally measured ones.

Since the identified matrices directly reflect the inherent properties of the structure, they can be naturally served as effective indices in SHM. In the simulated example, a specially designed artificial damage is applied on the FE model of a free-free conditional beam. The natural frequencies and FRFs are proved to be insensitive to the artificial damage, although the property of beam has been significantly changed. On the contrary, the identified system matrices are demonstrated to be capable of indicating the change of the structural properties, and thus they can be served as effective SHM indices in some special situation where the natural frequencies and FRFs are insensitive.

## 5. REFERENCES

- Balmès, E. (1997). "New Results on the Identification of Normal Modes From Experimental Complex Modes." *Mechanical Systems and Signal Processing*, 11(2), 229–243.
- Bernal, D., and Gunes, B. (2000). "Extraction of Second Order System Matrices From State Space Realizations." *14th ASCE Engineering Mechanics Conference*.
- Bi, S., Ouisse, M., and Foltête, E. (2018). "Probabilistic Approach for Damping Identification Considering Uncertainty in Experimental Modal Analysis." *AIAA Journal*, 1–12.
- Bi, S., Ouisse, M., Foltête, E., and Jund, A. (2017). "Virtual decoupling of vibroacoustical systems." *Journal of Sound and Vibration*, 401, 169–189.
- Carden, E. P., and Fanning, P. (2004). "Vibration based condition monitoring: A review." *Structural Health Monitoring*, 3(4), 355–377.
- Chang, K. C., and Kim, C. W. (2016). "Modal-parameter identification and vibration-based damage detection of a damaged steel truss

- bridge.” *Engineering Structures*, Elsevier Ltd, 122, 156–173.
- Lancaster, P., and Prells, U. (2005). “Inverse problems for damped vibrating systems.” *Journal of Sound and Vibration*, 283(3–5), 891–914.
- Lin, T. K., Hung, S. L., and Huang, C. S. (2012). “Detection of Damage Location Using a Novel Substructure-Based Frequency Response Function Approach With a Wireless Sensing System.” *International Journal of Structural Stability and Dynamics*, 12(04), 1250029.
- Yang, Y. B., Chang, K. C., and Li, Y. C. (2013). “Filtering techniques for extracting bridge frequencies from a test vehicle moving over the bridge.” *Engineering Structures*, 48, 353–362.
- Zhang, Q., and Lallement, G. (1987). “Comparison of normal eigenmodes calculation methods based on identified complex eigenmodes.” *Journal of Spacecraft and Rockets*, 24(1), 69–73.